Starch - Stärke

WILEY-VCH
Starch

RESEARCH ARTICLE OPEN ACCESS

Tannia Starch: Structural and Functional Characterization

Maria Dimopoulou[1] | Christos-Konstantinos Mouzakitis[2] | Costas G. Biliaderis[2] | Vassilis Kontogiorgos[3]

[1]School of Health and Life Sciences, Teesside University, Middlesbrough, UK | [2]Department of Food Science and Technology, School of Agriculture, Aristotle University of Thessaloniki, Thessaloniki, Greece | [3]Faculty of Land and Food Systems, The University of British Columbia, Vancouver, British Columbia, Canada

Correspondence: Maria Dimopoulou (M.Dimopoulou@tees.ac.uk)

Received: 21 May 2025 | **Revised:** 18 September 2025 | **Accepted:** 30 December 2025

Keywords: gelatinization | pasting | tannia starch | *Xanthosoma sagittifolium*

ABSTRACT

Tannia starch (*Xanthosoma sagittifolium*) is less characterized than other tropical tuber starches. This study analyzed the compositional, structural, thermal, and functional characteristics of crude and purified tannia starch to assess the impact of purification. Starches were examined using x-ray diffraction (XRD), proximate and particle size distribution analysis, scanning electron (SEM) and polarized light microscopy (PLM), pasting profile analysis, and differential scanning calorimetry (DSC). Proximate analysis showed minor differences between crude (CS) and purified (PS) starch preparations, indicating that tannia starch is fairly pure even in its crude form. Distinct differences were observed in pasting properties; CS (22% amylose) exhibited lower peak viscosity and setback, reflecting limited swelling and weaker retrogradation, whereas PS (28.5% amylose) displayed higher peak viscosity (2573 cP), greater breakdown, and a higher setback (820 cP), indicative of stronger swelling but reduced shear resistance. Both starch preparations had a mean granule size of ~3 μm and showed increased particle aggregation following extraction. XRD patterns revealed A-type crystallinity, while PLM indicated the loss of birefringence upon heating. Both starches exhibited similar gelatinization temperature (~83°C) as determined by DSC and pasting analysis. In conclusion, native-crystalline CS and PS provide pastes of enhanced viscosity and gel strength for functional applications.

1 | Introduction

Xanthosoma sagittifolium, commonly known as tannia, malanga, or new cocoyam, is a tropical tuber crop belonging to the Araceae family. Tannia is widely cultivated in tropical and subtropical regions, particularly in West Africa, the Caribbean, Central and South America, and Southeast Asia [1, 2]. It is grown for its edible corm and leaves, which serve as a food staple in these regions. Despite its importance, tannia still remains underutilized and less studied than other root and tuber crops like cassava, yam, or taro [3]. In particular, research on tannia starch has been limited, despite its unique physicochemical properties that could make it valuable for both food and industrial applications.

Tannia and taro are often called cocoyams due to their botanical similarities, agricultural importance, and widespread use in traditional diets [4]. Taro starch has been extensively studied and is appreciated for its small granule size, high digestibility, and functional properties, making it suitable for industrial applications [4, 5]. More specifically, taro's starch granules are small (1–8 μm) and exhibit A-type crystallinity, contributing to their high swelling power, rapid gelatinization, low setback viscosity, and easy digestibility, thereby making this starch desirable for a range of products [6]. Alternatively, tannia starch has distinct physicochemical characteristics that may offer advantages over taro starch in certain applications. Tannia starch granules are slightly larger (3–25 μm) and exhibit a polygonal morphology, which affects their pasting and gelatinization behavior [7].

This is an open access article under the terms of the Creative Commons Attribution License, which permits use, distribution and reproduction in any medium, provided the original work is properly cited.

© 2026 The Authors. *Starch - Stärke* published by Wiley-VCH GmbH

Compared to taro starch, tannia starch generally has higher pasting viscosity, greater gel stability, and resistance to enzymatic hydrolysis, which are sufficient to alter its functionality [8, 9]. Furthermore, tannia starch has been reported to have a higher gelatinization temperature and lower solubility, which may contribute to improved texture and stability in thermally processed food products [4].

Despite these promising attributes, the potential uses of tannia starch remain largely unexplored. Most research on tuber starches has focused on widely used sources, while tannia starch has received comparatively little attention. Additionally, while some previous work [1] has reported favorable pasting properties for tannia starch, there is still limited information on its molecular structure, amylose-to-amylopectin ratio, pasting behavior, and interactions with other food components. Comparative studies with taro and other starches remain scarce, making it difficult to fully assess its competitive advantages. The present study extends previous findings by explicitly comparing crude and purified tannia starch, highlighting how purification influences its structural, thermal, and functional behavior.

2 | Materials and Methods

2.1 | Materials

All reagents and chemicals utilized for determining amylose content were of analytical grade and were sourced from Sigma-Aldrich (St. Louis, MO, USA). Tannia tubers (~2.5 kg) were obtained from a local market in Nigeria (Noor Market).

2.2 | Starch Isolation

The starch isolation procedure is shown in Figure 1. Briefly, tannia tubers were manually peeled and washed with water, followed by grinding (De'Longhi, China) and oven-drying (GenLab, England) at 40°C for 2 h, yielding about 250 g (10% of fresh weight) of a crude starch (CS) preparation. This CS corresponds to a flour preparation that contains starch, along with other native corm constituents, and was used as a baseline for comparison with the purified starch (PS). CS powder was then mixed with water at a weight ratio of 1:3 (CS:water) and left under stirring for 1 h. The mixture was then filtered using a two-layered cheesecloth and allowed to pass through a sieve (90 μm). After filtration, the liquid was allowed to settle for 5 h. The settled starch was re-suspended in distilled water and centrifuged (Hettich Universal, Germany) at 4000 × *g* for 20 min at 25°C. The wet starch was oven-dried at 40°C for 2 h and gently pulverized, using a mortar and pestle, yielding approximately 80 g (3.2% of fresh weight; 32% of the crude flour) of a purified starch preparation (PS) [10]. Following extraction, proximate composition (moisture, ash, protein, fat, fiber, and carbohydrate content) of crude and purified tannia starches was determined externally at Beverley Analytical Laboratories, Hull, UK, using standard food analysis protocols.

2.3 | XRD Analysis

The dried samples (~5 g) were sieved through a 100 μm sieve and packed in a steel sample holder with a 27 mm diameter opening. Diffractograms were recorded with a Malvern-Panalytical Empyrean 3 x-ray diffractometer (Worcestershire, United Kingdom). Starch samples were scanned over the diffraction angle range of 5°–85° (2θ) at a scan speed of 4°/min and a step size of 0.04°, using a voltage of 45 kV and a current of 40 mA.

2.4 | Granule Morphology and Size Distribution Analysis

Starch samples were viewed by polarized light microscopy (Olympus Optical Co., Ltd., Tokyo, Japan). Starch granules (~100 mg) were suspended in 300 mg of distilled water, and a drop of the starch suspension was placed onto a glass slide. The slide was then covered with a coverslip and viewed under a BX63 microscope equipped with a DP23M camera and a BX-POL polarizer.

For scanning electron microscopy (SEM) imaging, a double-sided adhesive film was utilized to affix the starch granules to the stubs, which were subsequently subjected to gold sputter coating. Microscopic observations were conducted using a JSM-IT500 JEOL SEM apparatus (JEOL Ltd., Tokyo, Japan). The microscope was operated at an accelerating voltage of 20 kV [11].

The particle size distribution was analyzed using a Microtrac MRB particle analyzer (Microtrac Retsch GmbH, Germany). The samples were dispersed in water, and the refractive indices were set at 1.33 and 1.50 for water and starch, respectively [5].

2.5 | Differential Scanning Calorimetry

Starch gelatinization characteristics were evaluated using a DSC 3 calorimeter (Mettler-Toledo GmbH, Analytical, Zurich, Switzerland) as described by Kotsiou et al. [12]. About 14 mg of starch samples were mixed with distilled water (starch:water dispersions 30:70 w/w) and hermetically sealed into DSC stainless steel crucibles. The samples were then heated from 10°C to 120°C (heating rate 5°C/min). Onset temperature (T_o), peak temperature (T_p), conclusion temperature (T_c), and gelatinization enthalpy (ΔH) were recorded according to Biliaderis et al. [13]. All measurements were performed in triplicate.

2.6 | Starch Pasting

The pasting properties of each starch preparation (CS, PS) were assessed using a starch pasting cell in a rheometer (MCR 302 Anton Paar, Austria). A starch sample weighing 2.16 g was placed into the cell with 18 mL of distilled water. The mixture was then

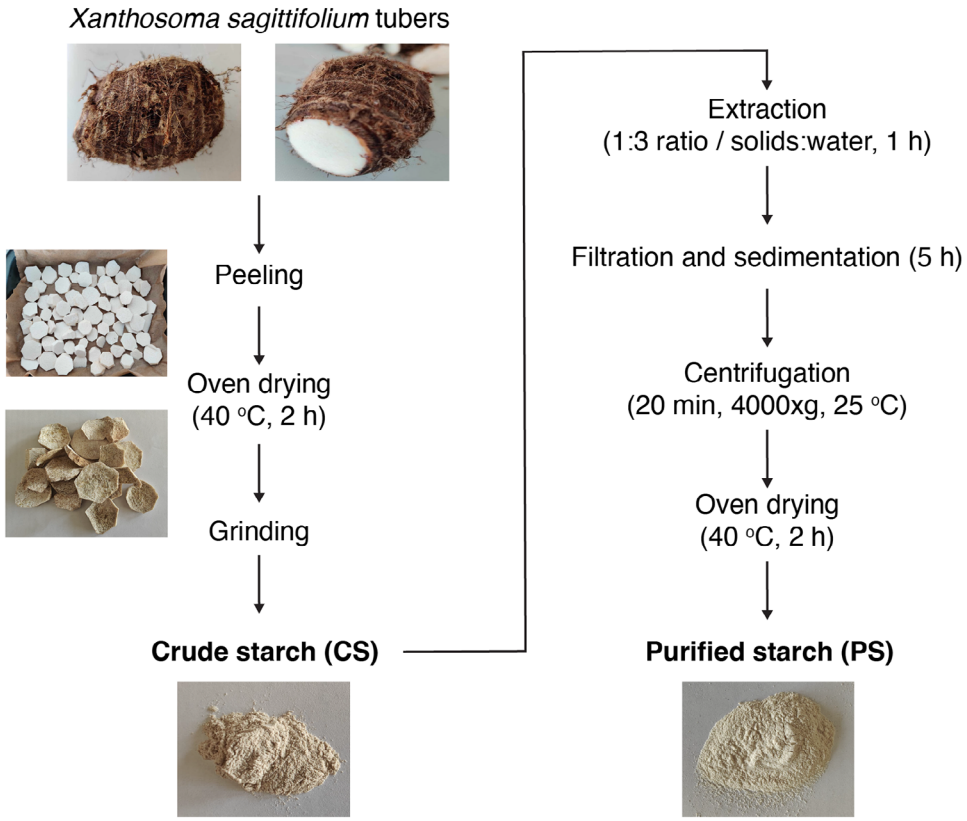


FIGURE 1 | Tannia starch isolation steps.

heated to 50°C and stirred at 960 rpm for 10 s to ensure a thorough starch dispersion. While maintaining a stirring speed of 160 rpm, the following temperature protocol was applied: maintaining initially the temperature at 50°C for 50 s, heating to 95°C over 450 s using a linear temperature ramp, holding at 95°C for 300 s, cooling to 50°C over 450 s using a linear temperature ramp, and finally maintaining the aqueous dispersion at 50°C for 120 s. The test was performed in triplicate for each sample.

2.7 | Amylose Content Determination

The amylose content of the starch samples was determined using a colourimetric method involving iodine complexation [14]. For this, 100 mg of the sample was wetted with 1 mL of 95% ethanol. The sample was then treated with 10 mL of 1 N NaOH, followed by heating in a water bath (Thermo Fisher Scientific, USA) at 90°C for 10 min to disperse the starch granules molecularly. Aliquots (5 mL) of diluted starch dispersions were neutralized and mixed with 1 mL diluted iodine reagent (0.002% I_2, 0.02% KI). The absorbance of the mixture was measured at 620 nm using amylose as a standard [14].

2.8 | Statistical Analysis

An unpaired *t*-test with Welch's correction was conducted at $\alpha = 0.05$ to analyze the data by Prism 10 statistical and graphing software (GraphPad Software, Boston, MA, USA) to compare the means of the evaluated parameters between the two starch preparations.

3 | Results and Discussion

3.1 | Compositional Analyses

Only minor differences were observed in proximate composition between crude and purified tannia starches (Table 1). This suggests that the crude starch was already relatively pure, and that the extraction–purification step primarily influenced functional and physicochemical attributes (e.g., apparent amylose content, pasting behavior, and thermal properties) rather than bulk composition, which is examined in detail in the following sections.

3.2 | XRD Analysis and Particle Morphology

Starch diffractograms (Figure 2) reveal the crystallinity of the samples before and after purification. The diffractograms exhibit distinct peaks at 2θ of 15°, 17°, 18°, and 23°, indicative of A-type crystallinity. This is typically observed with cereal and some tuber starches, including taro, yam, and cocoyam [15–17]. A-type crystallinity reflects a dense and ordered arrangement of amylopectin double helices, which form during starch biosynthesis under conditions of limited hydration [17]. Notably, the consistent presence of these peaks in the CS and PS samples demonstrates that the extraction process preserved the starch's intrinsic crystalline structure. In addition to these crystalline peaks, a broad scattering between 27° and 51° was observed, corresponding to the amorphous starch regions. The amorphous phase of granular starches represents the disordered regions

TABLE 1 | Pasting, thermodynamic properties, granule size, and amylose content of tannia starch before (CS) and after purification (PS). Values with a star (*) superscript indicate statistical significance at $p < 0.05$ within each row. Values with an ns are not statistically significant within each row.

	Crude starch (CS)	Purified starch (PS)
Moisture (% w/w)	9.9	11.3
Total fat/oil (% w/w)	0.6	0.6
Protein (% w/w)	7.4	6.6
Crude fiber (% w/w)	2.4	3.2
Ash (% w/w)	2.3	3.2
Total carbohydrates (%)	77.4	75.1
Peak viscosity (cP)	$1857.0^{*} \pm 99.4$	$2572.7^{*} \pm 162.1$
Pasting temperature (°C)	$82.3^{ns} \pm 1.2$	$82.6^{ns} \pm 0.9$
Holding strength (cP)	$1229.3^{*} \pm 18.1$	$582.1^{*} \pm 22.4$
Breakdown (cP)	$627.4^{*} \pm 82.3$	$1991.0^{*} \pm 140.0$
Final viscosity (cP)	$1863.3^{*} \pm 39.5$	$1403.0^{*} \pm 26.9$
Setback (cP)	$629.7^{*} \pm 56.7$	$820.3^{*} \pm 4.2$
Enthalpy (J/g)	$14.1^{ns} \pm 0.1$	$14.4^{ns} \pm 0.2$
DSC peak T (°C)	$83.7^{ns} \pm 0.1$	$82.8^{ns} \pm 0.3$
Glass transition temperature T_g (°C)	$62.5^{*} \pm 0.1$	$64.4^{*} \pm 0.1$
$d(1,0)$ (μm)	$3.1^{ns} \pm 0.1$	$3.3^{ns} \pm 0.3$
$d(4,3)$ (μm)	$334^{ns} \pm 48.2$	$302^{ns} \pm 29.6$
Apparent amylose content (%)	$22.7^{*} \pm 0.2$	$28.5^{*} \pm 0.8$

Note: 1 cP = 0.001 Pa s.

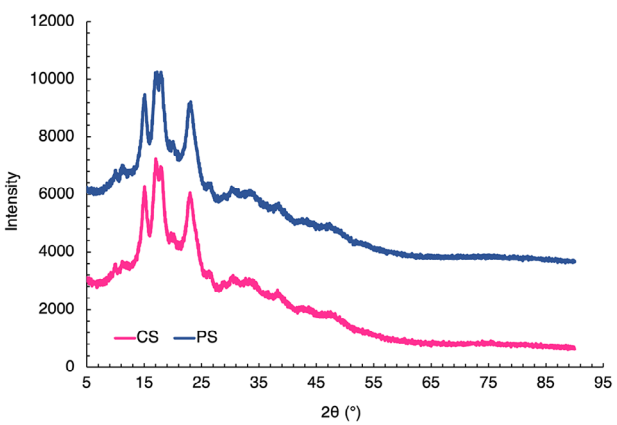


FIGURE 2 | X-ray diffractograms of crude (CS) and purified (PS) starch. Peaks at 15°, 17°, 18°, and 23° are indicative of A-type crystallinity.

of amylose and amylopectin molecules outside the crystalline domains in the granules [4].

Combining A-type crystalline entities, mostly assemblies of amylopectin short chains, with amorphous material is typical of some tuber-derived starches, such as those from taro (*Colocasia esculenta*) and yam (*Dioscorea* spp.) [6, 18]. Comparatively, studies on *X. sagittifolium* have also revealed dominant A-type diffraction patterns, with peaks 2θ around 15°, 17°, and 23° [9], similar to those noted in the present work. This structural similarity suggests that tannia starch shares comparable molecular packing and crystalline organization with starches from both *Colocasia* and *Xanthosoma* species. These features are related to moderate gelatinization temperatures of the granules, high water-binding capacity, and controlled enzymatic digestibility—functional traits that support applications in sauces, baby foods, and gelled systems [4, 16]. The preservation of A-type crystallinity following purification, alongside the existence of substantial amorphous material, reinforces tannia starch's potential for varying functionality. Overall, the structural profile aligns closely with that of well-characterized cocoyam starches, suggesting that tannia may also be utilized in a similar context.

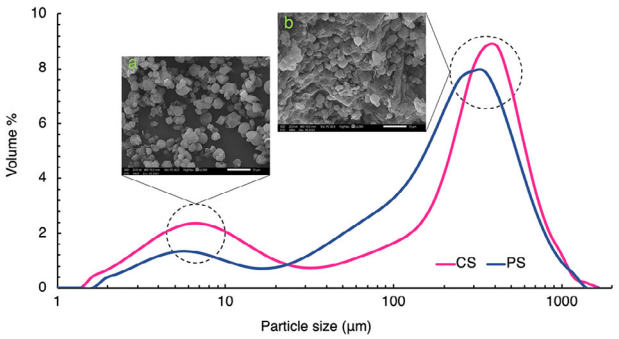


FIGURE 3 | Particle size distribution of crude (CS) and purified (PS) tannia starch preparations. Insets a and b show the SEM morphological features of granules present in the two starch preparations, corresponding to the respective peaks of the size distribution profiles; the scale bar is 10 μm.

The particle size distribution (Figure 3) for both tannia starch preparations, CS and PS, analyzed by laser diffraction, revealed a mean diameter of individual granules of approximately 3 μm ($d(1,0)$, Table 1). This value is consistent with previously reported data and closely concurs with the SEM findings (Figure 3, inset a), which show predominantly small, well-developed granules with polygonal to irregular surface morphology. The small granule size is characteristic of starches derived from aroids, particularly *Xanthosoma* and *Colocasia* species, and is markedly smaller than those from yam (*Dioscorea* spp., ~10–40 μm) or cassava starch (*Manihot esculenta*, ~8–30 μm) [5, 7, 19].

In addition to the peak at ~3 μm, the particle size distribution curves also showed the presence of a secondary population of larger particles (~300 μm, $d(4,3)$, Table 1) in both sample preparations, which may originate from partial aggregation of granules. This interpretation is supported by the SEM micrographs (Figure 3, inset b), where localized clusters of starch granules were noted. Such aggregation likely occurs during the drying of aqueous starch dispersions and/or due to their insufficient redispersion in aqueous media during measurements in the particle size analyzer, as has also been reported for other small granule-sized tuber starches, such as *Xanthosoma mafaffa* [20]. These aggregated clusters do not appear to result from inherent differences in granule size but rather from physical cohesion

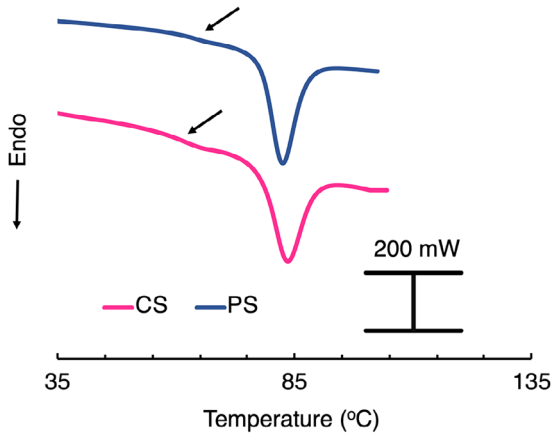


FIGURE 4 | DSC curves of tannia starch before (CS) and after purification (PS). Arrows indicate the presence of a smaller thermal event before the melting peak, typical of a glass transition (T_g).

between individual small-size granules, possibly mediated by residual surface components (e.g., residual amyloplast membrane material, proteins, etc.).

The coexistence of individual granules and clusters of granules explains the moderately heterogeneous particle size distribution profiles recorded, which may also influence the functional behavior of tannia starch in aqueous systems. For example, granule size and distribution heterogeneity can affect swelling uniformity, gelatinization rate, and susceptibility to shear-induced rupture of the granules [4, 6]. Notably, this profile aligns well with the high peak viscosity and increased breakdown values observed in the pasting analysis of aqueous dispersions, suggesting that rapid water uptake and granule swelling, partially facilitated by existing aggregated particles, are followed by significant granule disruption under shear [8, 9]. Similar rheological responses have also been reported for other tuber starches, including *Xanthosoma* and *Colocasia* species [18, 21], reflecting their granule structure organization, hydration dynamics, and paste stability. These rheological characteristics are functionally relevant, particularly for applications requiring high thickening power and controlled paste breakdown (e.g., gel-based formulations) [16].

3.3 | Thermal Properties

The apparent gelatinization enthalpies of the two starch preparations ranged between 14.1 and 14.4 J/g, showing no significant differences (Figure 4 and Table 1). These enthalpy values are in good agreement with those reported for other tuber starches, like yam (14.3–14.9 J/g), tapioca starch (13.5–14.3), sweet potato (12.9 J/g), and ginger (15.9 J/g), according to previous reports [22–26]. As can be seen in Table 1 and Figure 4, compared to other granular starches, the tannia starch preparations exhibited high peak gelatinization temperatures, with onset (T_o) at about 72°C and 74°C, peak (T_p) at 82.8°C and 83.7°C, and set (T_c) at 96°C and 97°C. Interestingly, these results indicate that the starch granules from tannia have more heat-stable crystallites compared to other starches from tubers or bulbs [24, 27, 28]. Peroni et al. [24] compared the properties of various tuber starches and found that cassava, arrowroot, and sweet potato starches exhibited lower onset gelatinization temperatures (61.5°C, 62.6°C, and 62.8°C, respectively) and enthalpy changes (10.4, 11.3, and 12.9 J/g, respectively). In contrast, yam and ginger starches gave the highest onset temperatures (70.7°C and 82.4°C, respectively) and enthalpy changes (14.3 and 15.9 J/g, respectively).

In general, starches classified as A-type, as in the case of tannia starch, exhibit higher gelatinization temperature since the A-type crystallites are thermodynamically more stable than their B- and C-type polymorphic counterparts [29, 30]. Additionally, amylopectin crystallites of higher chain lengths [31] and starch granules of relatively small size [32], such as those of tannia starch, could also contribute to its observed high gelatinization temperatures. Comparing DSC gelatinization data of native starches from various botanical sources is controversial because melting transition parameters are affected by factors like plant cultivar, environmental conditions during biosynthesis of starch granules, tissue source, extraction methods, thermal history, starch purity, heating rate, and water content in the heated dispersions, making direct comparisons complicated [31].

A closer examination of the DSC thermograms, particularly in the range of ~60–70°C (Figure 4, arrows), revealed the presence of a smaller thermal event, typical of a glass transition (T_g). Similar observations were also made by Biliaderis et al. [13] for some granular rice starches. This transition reflects a structural relaxation of the amorphous chain segments, that is, mediated by water, which acts as a plasticizer of the disordered starch chain segments [33]. This transition occurs before the melting of the crystalline regions of granular starch. Frequently, the anticipated discontinuity in the heat capacity function at T_g for amorphous polymers is not detectable by DSC for granular starch preparations (in heated aqueous dispersions) due to the coupling of the amorphous material with the crystalline regions [13, 31]. Actually, a range of non-ordered domains exists in granular starches, exhibiting varying plasticization responses by water or other small molecular weight co-solutes, and extending the glass-to-rubber transition over a broad range of temperatures, making this second-order state transition less detectable in the DSC traces. However, in the case of tannia starch, the high melting temperature of the crystallites makes it more feasible to observe the glass transition in the range of ~60–70°C under the hydration conditions adopted in the present work.

3.4 | Starch Pasting Characteristics and Amylose Content

The apparent amylose content of the CS preparation was 22% and increased to 28.5% following purification (PS). This change in amylose/amylopectin composition most likely reflects the removal of some non-starch components from the crude starch preparation upon starch extraction–purification. The amylose-to-amylopectin ratio of granular starches is a critical factor influencing gelatinization, viscosity development, and retrogradation, where an increased amylose content aligns with a higher hot paste and setback viscosity, as noted in the pasting profiles (Figure 5 and Table 1). Comparatively, tannia starch exhibits a moderate amylose content, similar to yam starch (27%–31%) but higher than cassava starch (17%–24%), which typically shows lower retrogradation tendencies [4, 19]. In addition, the pasting

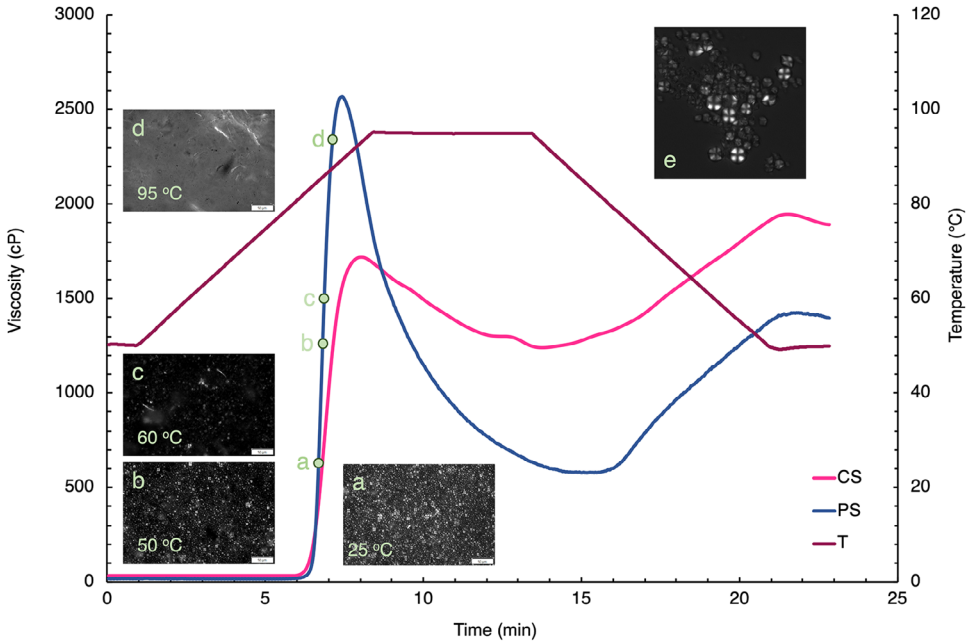


FIGURE 5 | Pasting curves of tannia starch preparations before (CS) and after purification (PS). Insets are polarized light microscopy (PLM) images of the granules upon heating: (a) PLM at 25°C, (b) PLM at 50°C, (c) PLM at 60°C, (d) PLM at 95°C, and (e) zoom in of native starch granules displaying the Maltese cross prior to heating; the scale bars in the light micrographs is 50 μm. The bright areas correspond to Maltese crosses that are gradually eliminated with increasing temperature. At 95°C, gelatinization is complete, accompanied by the absence of birefringence.

behavior of the purified tannia starch further supported its thermal characteristics, with a pasting temperature of 82.6°C (Figure 5). This value closely matched the gelatinization peak temperature of 82.8°C determined by DSC, indicating a strong alignment between functional swelling and thermal melting of the crystalline regions. Such correspondence suggests that granule swelling, viscosity development, and crystalline disruption occur simultaneously in heated aqueous dispersions of tannia starch, reflecting a more uniform and thermally coherent granule structure.

These observations contrast with many other tuber starches. For example, yam starch (*Dioscorea* spp.) typically shows a pasting temperature of 76–81°C, while its DSC peak temperature is often slightly higher, ranging from 84°C to 88°C [6, 19]. Similarly, taro starch (*C. esculenta*) exhibits pasting temperatures between 74°C and 78°C, with DSC endothermic peaks being typically around 82–85°C [7]. In these cases, pasting analysis usually demonstrates lower values than DSC due to the effects of shear and excess water during measurements. The consistency observed in tannia starch suggests that its crystalline domains may be more uniformly distributed or structurally integrated, leading to a single, well-defined transition point (from partially ordered to a disordered physical state) regardless of the method used to probe these transformations. Tannia starch's consistent pasting and DSC temperatures set it apart from other tropical tuber starches, potentially offering processing benefits like predictable thermal behavior and stable gelatinization under various conditions.

Peak viscosity reflects the starch's ability to form a hot paste upon heating and is a critical marker for swelling and granule integrity losses. The peak viscosity of the purified tannia starch was ~2573 cP, much higher than that of the CS preparation (Table 1). This suggests a greater capacity for water absorption and swelling. Hoover [4] has noted that starch granules with higher peak viscosity are more prone to disintegration due to weaker cohesive forces within the swollen granules. Applications requiring thick hot pastes (e.g., pie fillings with fruit pieces) benefit from higher peak viscosities. In comparison, lower viscosities are better suited for products that demand less thickening [8]. Such responses conform with the findings for tannia starch, which offers the dual advantage of forming strong hot pastes while remaining adaptable to various viscosity requirements.

Breakdown viscosity, defined as the difference between peak viscosity and holding strength (trough or minimum viscosity), provides an insight into the stability of swollen starch granules under applied thermal and shear forces [1]. PS exhibited a breakdown viscosity approximately three times greater than the CS (Table 1), indicating that while it undergoes extensive swelling, it is less resistant to shear-induced disintegration. This suggests weaker intermolecular and interparticle forces in the gelatinized starch dispersion. Starches with higher breakdown viscosity typically possess greater granule fragility, which may be attributed to lower phospholipid content or weaker hydrogen bonding within the partially crystalline starch matrix [6, 8].

The trough viscosity (or holding strength) represents the minimum viscosity attained after the peak, indicating the stability of swollen starch granules under prolonged heating under stirring. The PS exhibited values comparable to those reported for starch of *X. mafaffa* (Scoth), suggesting moderate thermal and shear degradation resistance [19]. The extent of viscosity retention at this stage is influenced by granule rigidity, amylose leaching (phase separation), and the formation of an entangled molecular network of starch chains.

Final viscosity represents the starch's ability to form a stable gel or paste upon cooling and reflects its retrogradation tendencies and textural stability. The setback viscosity is calculated as the difference between breakdown viscosity and final viscosity and provides insights into the starch's potential for gel formation and syneresis occurrence upon storage. The purified tannia starch exhibited a setback viscosity of ~820 cP, higher than the CS preparation, indicating a stronger tendency to retrograde and form firmer pastes. However, excessive retrogradation can lead to undesirable syneresis in frozen storage applications. The balance between gel firmness and storage stability positions tannia starch as a promising candidate for products requiring consistent texture over time [34]. The relationship between peak viscosity, breakdown viscosity, and final viscosity highlights the structural integrity of tannia starch granules, where the moderate amylose content and distinct granule morphology contribute to their pasting behavior. Additionally, the pasting properties are influenced by intergranular interactions, amylopectin chain length distribution, and the presence of phosphate groups, which can modulate swelling, shear resistance, and gelation kinetics [9, 31].

Polarized light microscopy was employed to further investigate the structural characteristics of the starches. The examination revealed distinct changes in the optical properties of starch granules upon heating, in agreement with the observed pasting temperature and peak viscosity data. Initially, the granules exhibited a typical birefringent pattern (Figure 5a,e), indicating the presence of partially crystalline entities within the polygonal to irregular granule morphology entities. As the temperature increased and the starch granules began to swell and gelatinize, the birefringence was reduced (Figure 5b,c), reflecting the disruption of the crystalline structure and the onset of gelatinization. The complete loss of birefringence (Figure 5d) at the peak pasting temperature (95°C) confirmed the end of the gelatinization process. This transition aligns with the high pasting temperature recorded for tannia starch, suggesting that the granules readily absorb water and swell, leading to a hot paste of significant viscosity. Overall, the polarized microscopy findings complement the pasting curve results, illustrating the relationship between the physical structure of tannia starch and its functional behavior.

To sum up, the minimal changes in proximate composition confirm that purification primarily affects some of the functional and structural properties of tannia starch rather than its bulk composition. The findings highlight tannia starch as a promising candidate for applications requiring viscosity development in food formulations, texture, and thermal stability. Future research should examine the storage behavior, modification strategies, and performance in real food and packaging systems, as well as scalability, to establish tannia starch as a competitive alternative to other granular starches of similar physical and functional properties.

4 | Conclusions

The present study provided a comprehensive evaluation of the composition, structure, and functionality of crude and purified tannia starch preparations. The findings demonstrated that purification led to notable modification in starch functionality, rather than in bulk composition, particularly by increasing amylose content and achieving higher viscosity, while maintaining the native A-type crystallinity, granular size, and polygonal granule morphology. The close agreement between pasting and DSC analyses, both of which show gelatinization around 83°C, highlights the predictable and coherent thermal behavior of tannia starch, reflecting a well-integrated granular structure. Overall, these findings establish tannia starch as a promising alternative source of granular starch with potential applications in the food industry and provide the foundation for future studies on its modification and performance in specific product systems.

Author Contributions

Maria Dimopoulou: conceptualization, investigation, formal analysis, writing – original draft, writing – review & editing, data curation, visualization. **Christos-Konstantinos Mouzakitis**: investigation, formal analysis, visualization, writing – original draft, writing – review & editing. **Costas G. Biliaderis**: investigation, formal analysis, visualization, writing – original draft, writing – review & editing. **Vassilis Kontogiorgos**: conceptualization, investigation, formal analysis, writing – original draft, writing – review & editing, data curation, visualization, funding acquisition.

Acknowledgments

V.K. is grateful for funding from the Canada Foundation for Innovation—John R. Evans Leaders Fund (Grant #: 44434).

Conflicts of Interest

The authors declare no conflicts of interest.

Data Availability Statement

The data that support the findings of this study are available on request from the corresponding author.

References

1. E. Pérez, F. S. Schultz, and E. P. de Delahaye, "Characterization of Some Properties of Starches Isolated From Xanthosoma sagittifolium (tannia) and Colocassia esculenta (taro)," *Carbohydrate Polymers* 60 (2005): 139–145.

2. J. P. Saikia and B. K. Konwar, "Physicochemical Properties of Starch From Aroids of North East India," *International Journal of Food Properties* 15 (2012): 1247–1261, https://doi.org/10.1080/10942912.2010.491929.

3. C. Mba and H. Agu, "Developments on the Bioactive Compounds and Food Uses of the Tubers: Colocasia esculenta (L) Schott (Taro) and Xanthosoma sagittifolium (L) Schott (Tannia)," *Asian Food Science Journal* 20 (2021): 101–112, https://doi.org/10.9734/afsj/2021/v20i1130380.

4. R. Hoover, "Composition, Molecular Structure, and Physicochemical Properties of Tuber and Root Starches: A Review," *Carbohydrate Polymers* 45 (2001): 253–267, https://doi.org/10.1016/S0144-8617(00)00260-5.

5. J. Jane, L. Shen, J. Chen, and S. Lim, "Physical and Chemical Studies of Taro Starches and flours1 2," *Cereal Chemistry* 69 (1992): 528–535.

6. S. N. Moorthy, "Physicochemical and Functional Properties of Tropical Tuber Starches: A Review," *Starch-Stärke* 54 (2002): 559–592, https://doi.org/10.1002/1521-379X(200212)54:12⟨559::AID-STAR2222559⟩3.0.CO;2-F.

7. M. Himeda, Y. Njintang, C. Gaiani, et al., "Physicochemical and Thermal Properties of Taro (*Colocasia esculenta* sp) Powders as Affected by State of Maturity and Drying Method," *Journal of Food Science and Technology* 51 (2014): 1857–1865, https://doi.org/10.1007/s13197-012-0697-9.

8. A. A. Boakye, M. Gudjónsdóttir, F. D. Wireko-Manu, et al., "Water–Starch Interactions of Red and White Cocoyam (*Xanthosoma sagittifolium*)," *Starch-Stärke* 71 (2019): 1800128.

9. S. Sukhija, S. Singh, and C. S. Riar, "Isolation of Starches From Different Tubers and Study of Their Physicochemical, Thermal, Rheological and Morphological Characteristics," *Starch-Stärke* 68 (2016): 160–168, https://doi.org/10.1002/star.201500186.

10. O. Yuliarti, E. Gusti, J. H. Chiang, P. X. Teo, and J. Y. Ng, "Rheological and Microstructural Properties of Native Cassava Starch-Low Methoxyl Pectin in a Fruit Filling Gel System," *LWT* 146 (2021): 111568, https://doi.org/10.1016/j.lwt.2021.111568.

11. C.-K. Mouzakitis, K. Kotsiou, G. Pontikakos, et al., "Unravelling the Structural Heterogeneity and Diversity in Rheological Behavior of Alkali-Extractable Wheat Bran Arabinoxylans Using Ammonia Pretreatment," *Food Hydrocolloids* 151 (2024): 109888, https://doi.org/10.1016/j.foodhyd.2024.109888.

12. K. Kotsiou, D.-D. Sacharidis, A. Matsakidou, C. G. Biliaderis, and A. Lazaridou, "Impact of Roasted Yellow Split Pea Flour on Dough Rheology and Quality of Fortified Wheat Breads," *Foods* 10 (2021): 1832, https://doi.org/10.3390/foods10081832.

13. C. G. Biliaderis, C. M. Page, T. J. Maurice, and B. O. Juliano, "Thermal Characterization of Rice Starches: A Polymeric Approach to Phase Transitions of Granular Starch," *Journal of Agricultural and Food Chemistry* 34 (1986): 6–14, https://doi.org/10.1021/jf00067a002.

14. F. L. Bates, D. French, and R. Rundle, "Amylose and Amylopectin Content of Starches Determined by Their Iodine Complex Formation1," *Journal of the American Chemical Society* 65 (1943): 142–148, https://doi.org/10.1021/ja01242a003.

15. A. A. Amanyunose, B. F. Olanipekun, and O. E. Adelakun, "Comparative Study on the Functional, Pasting and Physicochemical Properties of Native and Pregelatinized Cocoyam Starch (Xanthosoma sagittifolium)," *American Journal of Food Science and Technology* 4 (2025): 21–29, https://doi.org/10.54536/ajfst.v4i1.3889.

16. E. da Rosa Zavareze and A. R. G. Dias, "Impact of Heat-Moisture Treatment and Annealing in Starches: A Review," *Carbohydrate Polymers* 83 (2011): 317–328.

17. J. L. Jane, K. S. Wong, and A. E. McPherson, "Branch-Structure Difference in Starches of A-and B-type X-ray Patterns Revealed by Their Naegeli Dextrins," *Carbohydrate Research* 300 (1997): 219–227, https://doi.org/10.1016/S0008-6215(97)00056-6.

18. L. M. Nwokocha, N. A. Aviara, C. Senan, and P. A. Williams, "A Comparative Study of some Properties of Cassava (*Manihot esculenta*, Crantz) and Cocoyam (Colocasia esculenta, Linn) Starches," *Carbohydrate Polymers* 76 (2009): 362–367, https://doi.org/10.1016/j.carbpol.2008.10.034.

19. A. N. Ukom, P. C. Ojimelukwe, and J. M. Emetole, "Physicochemical and Functional Properties of Starch From Under-Utilized Yam (Dioscorea spp) and Cocoyam (Xanthosoma maffa (Scoth)) Tubers of Southeast Nigeria," *Starch-Stärke* 68 (2016): 410–415, https://doi.org/10.1002/star.201500114.

20. S. M. Londoño-Restrepo, N. Rincón-Londoño, M. Contreras-Padilla, et al., "Physicochemical, Morphological, and Rheological Characterization of Xanthosoma Robustum Lego-Like Starch," *International Journal of Biological Macromolecules* 65 (2014): 222–228.

21. A. M. Ogunmolasuyi, E. C. Egwim, M. A. Adewoyin, and O. Awoyinka, "A Comparative Study of Functional and Structural Properties of Starch Extracted From Dioscorea rotundata and Colocasia Esculenta," *Starch—Stärke* 68 (2016): 771–777, https://doi.org/10.1002/star.201500280.

22. C. Biliaderis, T. Maurice, and J. Vose, "Starch Gelatinization Phenomena Studied by Differential Scanning Calorimetry," *Journal of Food Science* 45 (1980): 1669–1674, https://doi.org/10.1111/j.1365-2621.1980.tb07586.x.

23. L. Chel-Guerrero, G. Cruz-Cervera, D. Betancur-Ancona, and J. Solorza-Feria, "Chemical Composition, Thermal and Viscoelastic Characterization of Tuber Starches Growing in the Yucatan Peninsula of Mexico," *Journal of Food Process Engineering* 34 (2011): 363–382, https://doi.org/10.1111/j.1745-4530.2009.00362.x.

24. F. Peroni, T. Rocha, and C. Franco, "Some Structural and Physicochemical Characteristics of Tuber and Root Starches," *Food Science and Technology International* 12 (2006): 505–513, https://doi.org/10.1177/1082013206073045.

25. R. Pongsawatmanit, P. Chantaro, and K. Nishinari, "Thermal and Rheological Properties of Tapioca Starch Gels With and Without Xanthan Gum Under Cold Storage," *Journal of Food Engineering* 117 (2013): 333–341, https://doi.org/10.1016/j.jfoodeng.2013.03.010.

26. D. Thirathumthavorn and T. Trisuth, "Gelatinization and Retrogradation Properties of Native and Hydroxypropylated Crosslinked Tapioca Starches With Added Sucrose and Sodium Chloride," *International Journal of Food Properties* 11 (2008): 858–864, https://doi.org/10.1080/10942910701659567.

27. K. Thitipraphunkul, D. Uttapap, K. Piyachomkwan, and Y. Takeda, "A Comparative Study of Edible Canna (Canna edulis) Starch From Different Cultivars. Part I. Chemical Composition and Physicochemical Properties," *Carbohydrate Polymers* 53 (2003): 317–324, https://doi.org/10.1016/S0144-8617(03)00081-X.

28. P. Van Hung and N. Morita, "Physicochemical Properties of Hydroxypropylated and Cross-Linked Starches From A-Type and B-Type Wheat Starch Granules," *Carbohydrate Polymers* 59 (2005): 239–246, https://doi.org/10.1016/j.carbpol.2004.09.016.

29. P. J. Jenkins, R. E. Cameron, and A. M. Donald, "A Universal Feature in the Structure of Starch Granules From Different Botanical Sources," *Starch—Stärke* 45 (1993): 417–420, https://doi.org/10.1002/star.19930451202.

30. Y. Sun, M. Wang, S. Ma, and H. Wang, "Physicochemical Characterization of Rice, Potato, and Pea Starches, Each With Different Crystalline Pattern, When Incorporated With Konjac glucomannan," *Food Hydrocolloids* 101 (2020): 105499, https://doi.org/10.1016/j.foodhyd.2019.105499.

31. C. G. Biliaderis, "Structural Transitions and Related Physical Properties of starch," in *Starch: Chemistry and Technology*, 3rd ed., ed. R. L. Whistler and J. N. BeMiller (Elsevier—Academic Press, 2009), 293–372.

32. X. Peng and Y. Yao, "Small-Granule Starches From Sweet Corn and Cow Cockle: Physical Properties and Amylopectin Branching Pattern," *Food Hydrocolloids* 74 (2018): 349–357, https://doi.org/10.1016/j.foodhyd.2017.08.025.

33. L. Slade, H. Levine, and D. S. Reid, "Beyond Water Activity: Recent Advances Based on an Alternative Approach to the Assessment of Food Quality and Safety," *Critical Reviews in Food Science & Nutrition* 30 (1991): 115–360, https://doi.org/10.1080/10408399109527543.

34. K. O. Falade and C. A. Okafor, "Physical, Functional, and Pasting Properties of Flours From Corms of Two Cocoyam (Colocasia esculenta and Xanthosoma sagittifolium) Cultivars," *Journal of Food Science and Technology* 52 (2015): 3440–3448.